The Astrophysical Journal, 651:L89–L92, 2006 November 10


# ESCAPE OF IONIZING RADIATION FROM STAR-FORMING REGIONS IN YOUNG GALAXIES

Alexei O. Razoumov[1] and Jesper Sommer-Larsen[2]

*Received 2006 August 31; accepted 2006 September 22; published 2006 October 23*

## ABSTRACT

Using results from high-resolution galaxy formation simulations in a standard ΛCDM cosmology and a fully conservative multiresolution radiative transfer code around point sources, we compute the energy-dependent escape fraction $f_{esc}$ of ionizing photons from a large number of star-forming regions in two galaxies at five different redshifts from $z = 3.8$ to 2.39. All escape fractions show a monotonic decline with time, from (at the Lyman limit) ~6%–10% at $z = 3.6$ to ~1%–2% at $z = 2.39$, due to higher gas clumping at lower redshifts. It appears that increased feedback can lead to higher $f_{esc}$ at $z \gtrsim 3.4$ via the evacuation of gas from the vicinity of star-forming regions and to lower $f_{esc}$ at $z \lesssim 2.39$ through the accumulation of swept-up shells in denser environments. Our results agree well with the observational findings of Inoue et al. on the redshift evolution of $f_{esc}$ in the redshift interval $z = 2$–3.6.

*Subject headings:* galaxies: formation — intergalactic medium — H II regions — radiative transfer

*Online material:* color figures

## 1. INTRODUCTION

In the redshift interval $2 < z < 6$, most ionizing photons in the universe are thought to originate in Population II stars in normal ($V_c \gtrsim 30$–50 km s$^{-1}$) galaxies (Nagamine et al. 2006). For reionization calculations at $z > 6$, photons from lower mass halos should be taken into account (Iliev et al. 2006a), whereas at $z \sim 2$, active galactic nuclei start to play a dominant role (Madau et al. 1999). The fact that the metagalactic UV field peaks at $2 < z < 4$ (Inoue et al. 2006 and references therein) points to a peak in the galactic star formation (SF) rate at such redshifts (see also Panter et al. 2006). A major uncertainty in modeling the effect of this SF on the thermal state of the intergalactic medium (IGM) is the value of the escape fraction $f_{esc}$ of ionizing UV photons, which is a function of redshift, galaxy type, and mass.

The best observational estimates of $f_{esc}$ come from the detailed multi–wave-band studies of the local universe. Leitherer et al. (1995) find that less than 3% of ionizing photons from low-redshift starburst galaxies escape into the IGM. More recently, for several local starburst galaxies, Heckman et al. (2001) estimate $f_{esc} \lesssim 6\%$, noting that inclusion of dust will further reduce $f_{esc}$, and Bergvall et al. (2006) find $f_{esc} \sim 4\%$–10% for another local starburst.

The situation is markedly different at $z \gtrsim 3$, where the Lyman continuum (LyC) detection points at much higher $f_{esc}$ (Steidel et al. 2001). By comparing the direct observations of the LyC from galaxies to the mean cosmic UV background (UVB) intensity, Inoue et al. (2006) conclude that the average $f_{esc}$ increases from 1%–2% at $z = 2$ to ~10% at $z \gtrsim 3.6$.

Most theoretical estimates of $f_{esc}$ to date have been based on models with a smooth distribution of gas (Ricotti & Shull 2000) or semianalytical models with expanding shells and superbubbles in a disk galaxy (Dove et al. 2000; Fujita et al. 2003). Recently, Alvarez et al. (2006) computed $f_{esc}$ around the first stars at $z = 20$ with three-dimensional (3D) ray-tracing focusing on the effect of ionizing photons on nearby halos. However, $f_{esc}$ at lower redshifts is an entirely different quantity, due to very different conditions for star formation, higher gas clumping, and lower Population II stellar masses. In this Letter we present ab initio calculations of the energy-dependent $f_{esc}$ of ionizing radiation from SF regions in protogalaxies found in numerical simulations at five different redshifts from $z =$ 2.39 to 3.8. We define $f_{esc}(\nu, r)$ simply as a fraction of photons of energy $h\nu$ that reach a shell of radius $r$ around a given source; by definition, $f_{esc}(\nu, 0) = 1$. We postprocess high-resolution simulation data sets with radiative transfer (RT) on nested grids, with a maximum grid resolution of 15 pc. Each galaxy contains from several hundred to several thousand distinct stellar sources representing individual, young SF regions. Our interstellar gas distribution is extremely clumpy due to an array of physical processes including feedback from SF. We also estimate the effect of the dynamical expansion of H II regions on the escape of ionizing photons.

## 2. THE CODE AND MODELS

To compute the escape of ionizing radiation from SF regions, we use an extension of the fully threaded transport engine (FTTE; Razoumov & Cardall 2005) to point sources. This new module was previously briefly introduced in the comparison study by Iliev et al. (2006b). It extends the adaptive ray-splitting scheme of Abel & Wandelt (2002) to a model with variable grid resolution. Sources of radiation can be hosted by cells of any level of refinement, although usually in cosmological applications sources are sitting on the deepest level of refinement (Fig. 1). Around each point source, we build a system of $12 \times 4^{n-1}$ radial rays that split either when we move farther away from the source or when we enter a refined cell, and $n = 1, 2, \ldots,$ is the angular resolution level. Once a radial ray is refined, it stays refined, even if we leave the high spatial resolution patch, until even further angular refinement is necessary. All ray segments are stored as elements of their host cells, and for actual transport we just follow these interconnected data structures, accumulating photoreaction number and energy rates in each cell. With multiple sources, we add the rates from all sources before updating the time-dependent rate network using the chemistry solver from Abel et al. (1997),

[1] Institute for Computational Astrophysics, Department of Astronomy and Physics, Saint Mary's University, Halifax, NS B3H 3C3, Canada; razoumov@ap.smu.ca.

[2] Dark Cosmology Centre, Niels Bohr Institute, University of Copenhagen, Juliane Maries Vej 30, DK-2100 Copenhagen, Denmark; jslarsen@dark-cosmology.dk.

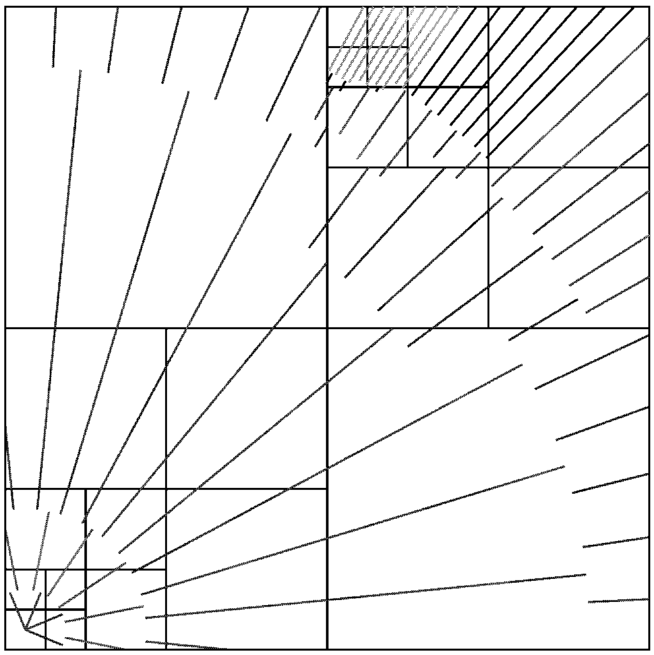

FIG. 1.—Radial ray geometry in the FTTE point-source algorithm. To avoid a nonuniform coverage of a cell such as that seen at the top of this box, we normally avoid cell interfaces with a jump in refinement by more than one level. [*See the electronic edition of the Journal for a color version of this figure.*]

and the global time step is chosen such that each species abundance does not change by more than 30%.

With a small ($N_{src} < 10^3$) number of star particles, we can compute a full ray geometry separately for each source. For a large number of sources ($10^3$–$10^6$), the algorithm allows for the construction of trees of sources in which individual tree nodes are treated as a single source far from its origin.

Our algorithm shares many common ideas with the recent RT module of the cosmological structure formation code Enzo implemented by Abel et al. (2006) to study feedback from Population III stars and, in fact, is the basis of an independently developed radiation hydrodynamics module of Enzo that we will introduce elsewhere.

### 2.1. *Galaxy Formation Models*

We use results of high-resolution galaxy formation simulations in a standard ΛCDM cosmology done with a significantly improved version of the TreeSPH code described by Sommer-Larsen et al. (2003)—some detail is given in Sommer-Larsen (2006). The simulations invoke the formation of discrete star "particles," which represent a population of stars born at the same time in accordance with a given initial mass function (IMF). For the purpose of this work, we focus on two (proto-) galaxies, K15 and K33, which at $z = 0$ become typical disk galaxies of $V_c = 245$ and 180 km s$^{-1}$, respectively. The RT calculations are performed at five different redshifts, $z = 3.8$, 3.6, 3.4, 2.95, and 2.39, for "normal" resolution simulations and at the first three of those redshifts for "high" resolution simulations (8 times higher mass resolution, twice better force resolution). For galaxy K15, we also vary the strength of supernova (SN) feedback (Table 1). Total particle numbers range from $\sim 1.6 \times 10^5$ to $\sim 2.2 \times 10^6$; star (and smoothed particle hydrodynamics [SPH]) particle masses are $1.1 \times 10^6$ and $1.4 \times 10^5$ $M_\odot$ for normal and high-resolution simulations, respectively.

Radiative transfer is computed on top of a nested data structure containing 3D distributions of physical variables. To create such a structure from the SPH simulation data sets, for each galaxy we cut out a (250 kpc)$^3$ box centered on the galaxy and projected this box onto a $128^3$ uniform grid. We then subdivided every base grid cell containing more than $N_{max} = 10$ SPH particles and continued this process of subdivision recursively so that no cell contains more than $N_{max}$ gas particles.

TABLE 1
NUMBER OF DISTINCT STAR PARTICLES OF AGE ≤34 Myr

| Simulation | Resolution | Feedback | Redshift 3.8 | 3.6 | 3.4 | 2.95 | 2.39 |
|---|---|---|---|---|---|---|---|
| Galaxy 1 | | | | | | | |
| K15-1-8 ......... | Normal | >Normal | ... | 347 | ... | 1000 | 560 |
| K15-06-8 ....... | Normal | Normal | 431 | 560 | 595 | 1161 | 596 |
| K15-06-64 ...... | High | Normal | 5061 | 5248 | 6005 | ... | ... |
| Galaxy 2 | | | | | | | |
| K33-06-8 ....... | Normal | Normal | 306 | 340 | 390 | 337 | 144 |
| K33-06-64 ...... | High | Normal | 2566 | 3122 | 3389 | ... | ... |

### 2.2. *Stellar Population Synthesis*

In the (normal resolution) galaxy K15-1-8 at $z = 3.6$, there are 347 stellar sources younger than $t_{up} = 34$ Myr (Fig. 2). The birth times of particles are distributed almost uniformly over the span of 34 Myr, corresponding to a nearly constant star formation rate (SFR) of 11.6 $M_\odot$ yr$^{-1}$. To compute the stellar UV luminosity function for this and other galaxies, we use the population synthesis package Starburst1999 (Leitherer et al. 1999) with continuous SF at a constant rate of 11.6 $M_\odot$ yr$^{-1}$ distributed among 347 stars. For other galaxies and at other redshifts, the SFR per particle is adjusted to account for the actual number of stars produced in the past 34 Myr, and the specific (per unit spectrum) luminosity is distributed uniformly among all stars in the volume.

We assume a triple-interval Arimoto-Yoshii–like IMF with

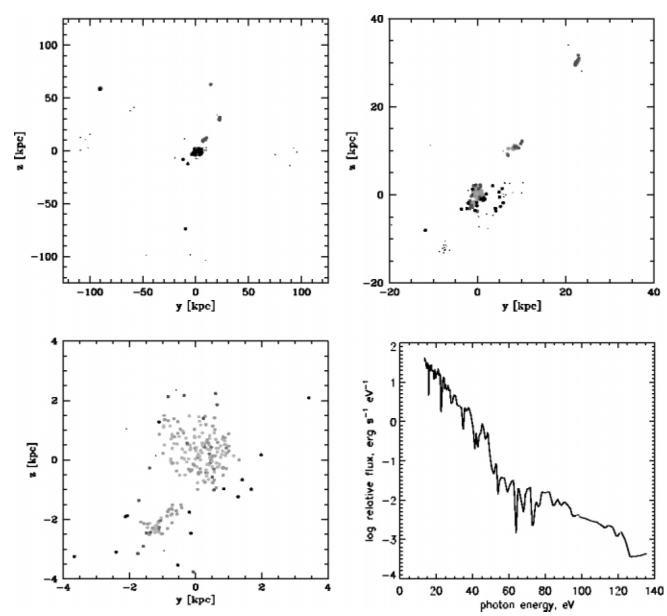


FIG. 2.—Distribution of all stellar particles (SF regions) younger than $t_{up} = 34$ Myr in the volumes 250 kpc (*top left*), 60 kpc (*top right*), and 8 kpc (*lower left*) on a side centered on the galaxy K15-1-8 at $z = 3.6$. The shade of each particle represents the level of the host cell. The lower right panel shows the input spectrum of a star particle. [*See the electronic edition of the Journal for a color version of this figure.*]

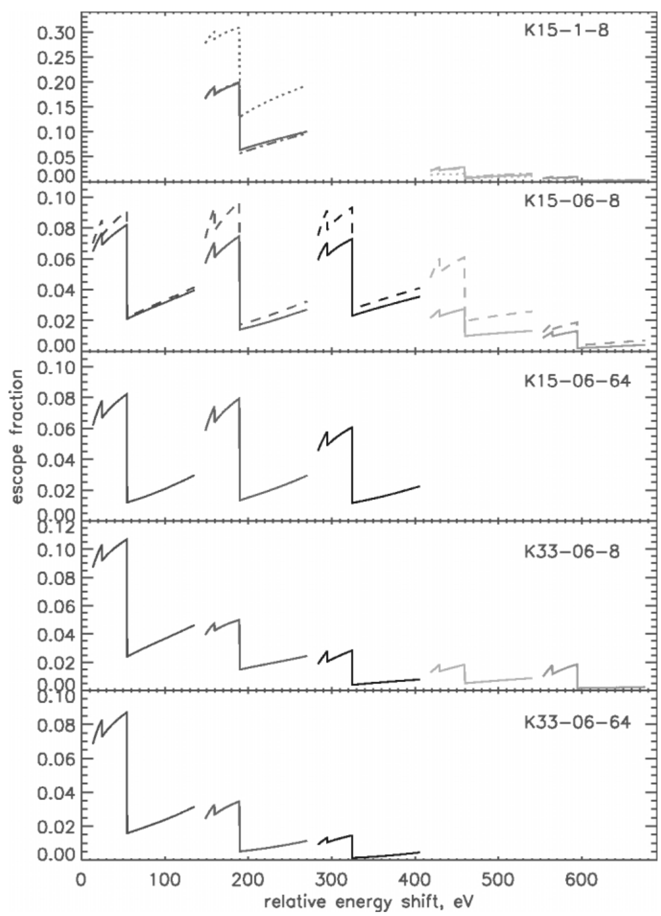


FIG. 3.—Spectral dependence of $f_{esc}$ at $r = 100$ kpc for all five input galaxy models at (where transfer has been computed) $z = 3.8$, $z = 3.6$, $z = 3.4$, $z = 2.95$, and $z = 2.39$ (*from left to right in each panel*). For each model, the redshift evolution is from left to right, and each curve goes from 13.6 to 135 eV. All solid lines are models without the H II region expansion, with the SFR distributed uniformly among all stars younger than 34 Myr. For K15-06-8, the dashed lines show models with the H II region expansion. For K15-1-8, we also computed the models with the *same* SFR distributed among stars younger 3.4 Myr (*dotted lines*) and 10 Myr (*dash-dotted lines*). [*See the electronic edition of the Journal for a color version of this figure.*]

indices 0.5, 1.2, and 1.7 above the mass boundaries of 0.1, 0.5, and 1 $M_\odot$, respectively, a supernova cutoff at 8 $M_\odot$, a black hole cutoff at 120 $M_\odot$, and solar metallicity. The resulting spectrum is shown in the lower right panel of Figure 2.

### 2.3. *Heating and* H II *Region Expansion*

The TreeSPH code assumes the UVB of Haardt & Madau (1996) with self-shielding in regions in which the mean free path of Lyman limit photons is less than 1 kpc. In addition to radiative heating and cooling and the hydrodynamical $P\,dV$ term, some heating originates from shock dissipation that we include in the following way.

After we project the 3D hydro fields onto the grids, in each cell we apply the uniform UVB with the self-shielding correction and compute the amount of additional heating needed to keep the temperature of that cell constant (thermal equilibrium without sources). We then switch on the stellar sources retaining the extra heating term and evolve simultaneously the equations of point-source transfer and nonequilibrium chemistry to 10 Myr. With continuous SF and constant UV luminosities, all $f_{esc}$ reach a plateau after the first few megayears. In this Letter all results are presented at $t = 10$ Myr, at which point we assume convergence.

Direct momentum transfer from UV photons to the interstellar/intergalactic gas is negligible (Spitzer 1978; Whalen & Norman 2006). However, heating and ionization by stellar photons create pressure gradients that drive the expansion of the H II regions into the surrounding gas. The physics of expansion has been studied in detail in 1D (Kitayama et al. 2004; Whalen & Norman 2006), 2D (Shapiro et al. 2004), and recently 3D (Abel et al. 2006) radiation hydrodynamics simulations. Without coupling RT to the hydro code, we cannot model this expansion self-consistently. However, we can mimic its effect by lowering the density in the giant H II region around the starburst region, which will ease the escape of UV photons. We use the results from § 3.1 of Larsen et al. (2001), which lists the "initial Strömgren radius" $R_0$ (1 Myr after the burst) and the "final Strömgren sphere" $R_e$ (4 Myr after the burst; at this time the UV luminosity declines rapidly) as functions of the local density and the ionizing source luminosity.

For each source, we use the initial gas density $n_0^{src}$ of the its host cell to find $R_0$ and $R_e$ and then modify the density of each cell inside $R_e$ by $n_e^{src}/n_0^{src}$, provided that the initial density of that cell $n_0 \le n_0^{src}$. For $n_0 > n_0^{src}$, the expanding shell hits a denser region, and without a full hydrodynamical calculation one cannot predict whether this will lead to expansion or compression of the denser region, which explains our condition. Therefore, for a given source, our density correction is anisotropic, which seems entirely realistic for an H II front expansion in an inhomogeneous medium.

For such large galaxies, we do not expect our results to change significantly if a fully self-consistent hydro/RT approach is used, as the energetic and momentum effects of ionization fronts are negligible compared to the effects of Type II SN explosions, shocks, etc., which are already included into our models, resulting in a very clumpy interstellar medium (ISM). However, the radiative feedback would also smooth some of the small-scale structure by raising the Jeans mass, which is especially important in lower mass galaxies, an effect that we plan to include in our future simulations.

## 3. RESULTS AND DISCUSSION

Figure 3 shows the spectral dependence of $f_{esc}$ at $r = 100$ kpc in each model, averaged over all sources. All $f_{esc}$ have been corrected for the boundary of the volume. For individual sources, the escape of photoionizing radiation is similar to a phase transition: it is very sensitive to conditions at the source and therefore can vary by a sizable factor for the same galaxy over the course of its evolution. We find that while there are variations among the models, the escape fractions tend to decrease with lower redshift, reflecting the fact that with time more gas cools into the higher density clouds, and that the SFR declines at $z < 2.95$. With normal feedback in both galaxies, $f_{esc}$ at the Lyman edge drops from 8%–10% at $z = 3.8$ to ~1%–2% at $z = 2.39$.

Not surprisingly, in all our models, the $f_{esc}$ of photons capable of doubly ionizing helium is very low, due to the softness of stellar radiation. The escape fraction of photons capable of single He ionization is comparable at all redshifts to that of H-ionizing photons.

Increasing SN feedback in K15 evacuates more gas from the vicinity of the SF regions, leading to a threefold rise in $f_{esc}$ at $z = 3.6$. Lower local gas densities translate into a 40% reduction in the SFR (Table 1). At $z = 2.95$, a denser environment near the sources produces a much smaller difference in the SFR and $f_{esc}$, when we increase the strength of feedback, and, at $z = 2.39$, $f_{esc}$ actually drops by 25% as a larger fraction of gas swept up by the shocks stays in the vicinity of the SF regions.

Next we compare our normal and high-resolution results, at $z = 3.8$–3.4, and find a good agreement between the two. We see it as an additional test of our algorithm, since other properties of the two sets of simulations (SFR, etc.) also match.

Since our choice of distributing SF over the $t_{up} = 34$ Myr youngest stars is somewhat arbitrary, in galaxy K15-1-8 we also experimented with the same amount of SF distributed over all stars younger than $t_{up} = 10$ and 3.4 Myr. Ideally, these young stars would produce most of the ionizing UV photons. Since we do not calculate transfer and hydro simultaneously, we feel that applying continuous SF with the constant rate is a better computational approach than assuming instantaneous SF, which will have no lasting effect on the thermal state of the IGM after a few megayears. With continuous SF, we expect our results to converge as we increase the number of star particles. The results at $t_{up} = 10$ and 34 Myr are in fact very close to each other at all three redshifts (Fig. 3), whereas the 3.4 Myr results are somewhat off, likely related to the small number of sources used to represent the SF in this latter case.

The dashed lines in K15-06-8 in Figure 3 show the energy-dependent $f_{esc}$ at $r = 100$ kpc corrected for the H II region expansion. At most redshifts, expansion raises $f_{esc}$ by 10%–30%, although at $z = 2.95$, $f_{esc}$ jumps by more than a factor of 2. Further analysis shows that most of this change can be attributed to the removal of the gas from the highest refinement level cells that are hosting the sources, not the surrounding cells.

Using galaxy K15-1-8 at $z = 3.6$ as an example, we can examine how $f_{esc}$ changes with distance from sources. A large fraction of photons reaches the radius $r = 100$ pc. As we do not have any reliable information on gas clumping on subresolution scales at these redshifts, the effective radius of absorption is not firmly established at this point. In our current models, most absorption occurs within a few hundred parsecs of each star particle, well inside the virial radius of ∼45 kpc. At $z = 3.6$, the protogalaxy consists of several star-forming regions as well as a significant amount of the intergalactic H I, all of which account for some fractional absorption beyond 1 kpc.

In this study, we neglected the effect of dust extinction. Benson et al. (2006) point out that in the case of a smooth ISM, attenuation by dust can reduce $f_{esc}$ by a factor of a few. For a clumpy ISM at high redshifts, the magnitude of dust attenuation should be much lower, particularly when most ionizing photons are produced in starbursts as opposed to quiescent disks.

In conclusion, our models with an exact ionizing continuum RT around a large number of SF regions in young protogalaxies show a monotonic decline in $f_{esc}$ of ionizing photons from higher to lower redshifts. With the normal feedback strength, $f_{esc}$ at the Lyman edge drops from ∼6%–10% at $z = 3.6$ to ∼1%–2% at $z = 2.39$. At higher redshifts, SF on average occurs at slightly lower densities, resulting in an easier escape of UV photons into the IGM. This result agrees well with the observational findings of Inoue et al. (2006) on the redshift evolution of $f_{esc}$. Note that although the two galaxies in our study have a mass ratio of ∼2.5, their $f_{esc}$ are very similar. One could suggest perhaps that once star formation begins, it is the physical conditions in the clumpy gas clouds that determine the escape of UV photons, rather than the overall properties of their host galaxies. However, one would need a much larger statistical sample to test this speculation. In our next paper we will further examine the role of the fine structure of the clumpy ISM in the escape of ionizing photons as well as the importance of hydrodynamical effects.

We wish to thank the referee for some very constructive feedback. A. O. R. would like to thank Mika Juvela and Eric Lentz for valuable discussions on numerical methods, as well as the hospitality of the Dark Cosmology Centre at the University of Copenhagen. The TreeSPH simulations were performed on the SGI Itanium II facility provided by DCSC. The Dark Cosmology Centre is funded by the DNRF.

## REFERENCES

Abel, T., Anninos, P., Zhang, Y., & Norman, M. L. 1997, NewA, 2, 181
Abel, T., & Wandelt, B. D. 2002, MNRAS, 330, L53
Abel, T., Wise, J. H., & Bryan, G. L. 2006, ApJL, submitted (astro-ph/0606019)
Alvarez, M. A., Bromm, V., & Shapiro, P. R. 2006, ApJ, 639, 621
Benson, A. J., Sugiyama, N., Nusser, A., & Lacey, C. G. 2006, MNRAS, 369, 1055
Bergvall, N., Zackrisson, E., Andersson, B.-G., Arnberg, D., Masegosa, J., & Östlin, G. 2006, A&A, 448, 513
Dove, J. B., Shull, J. M., & Ferrara, A. 2000, ApJ, 531, 846
Fujita, A., Martin, C. L., Mac Low, M.-M., & Abel, T. 2003, ApJ, 599, 50
Haardt, F., & Madau, P. 1996, ApJ, 461, 20
Heckman, T. M., Sembach, K. R., Meurer, G. R., Leitherer, C., Calzetti, D., & Martin, C. L. 2001, ApJ, 558, 56
Iliev, I. T., Mellema, G., Shapiro, P. R., & Pen, U.-L. 2006a, MNRAS, submitted (astro-ph/0607517)
Iliev, I. T., et al. 2006b, MNRAS, 371, 1057
Inoue, A. K., Iwata, I., & Deharveng, J.-M. 2006, MNRAS, 371, L1
Kitayama, T., Yoshida, N., Susa, H., & Umemura, M. 2004, ApJ, 613, 631
Larsen, T. I., Sommer-Larsen, J., & Pagel, B. E. J. 2001, MNRAS, 323, 555
Leitherer, C., Ferguson, H. C., Heckman, T. M., & Lowenthal, J. D. 1995, ApJ, 454, L19
Leitherer, C., et al. 1999, ApJS, 123, 3
Madau, P., Haardt, F., & Rees, M. J. 1999, ApJ, 514, 648
Nagamine, K., Cen, R., Furlanetto, S. R., Hernquist, L., Night, C., Ostriker, J. P., & Ouchi, M. 2006, NewA Rev., 50, 29
Panter, B., Jimenez, R., Heavens, A. F., & Charlot, S. 2006, MNRAS, submitted (astro-ph/0608531)
Razoumov, A. O., & Cardall, C. Y. 2005, MNRAS, 362, 1413
Ricotti, M., & Shull, J. M. 2000, ApJ, 542, 548
Shapiro, P. R., Iliev, I. T., & Raga, A. C. 2004, MNRAS, 348, 753
Sommer-Larsen, J. 2006, ApJ, 644, L1
Sommer-Larsen, J., Götz, M., & Portinari, L. 2003, ApJ, 596, 47
Spitzer, L. 1978, Physical Processes in the Interstellar Medium (New York: Wiley-Interscience)
Steidel, C. C., Pettini, M., & Adelberger, K. L. 2001, ApJ, 546, 665
Whalen, D., & Norman, M. L. 2006, ApJS, 162, 281